



**HAL**  
open science

**Potential and limitations of on-line comprehensive reversed phase liquid chromatographyxsupercritical fluid chromatography for the separation of neutral compounds: An approach to separate an aqueous extract of bio-oil**

Morgan Sarrut, Amélie Corgier, Gérard Crétier, Agnès Le Masle, Stéphane Dubant, Sabine Heinisch

► **To cite this version:**

Morgan Sarrut, Amélie Corgier, Gérard Crétier, Agnès Le Masle, Stéphane Dubant, et al.. Potential and limitations of on-line comprehensive reversed phase liquid chromatographyxsupercritical fluid chromatography for the separation of neutral compounds: An approach to separate an aqueous extract of bio-oil. *Journal of Chromatography A*, 2015, 1402, pp.124-133. 10.1016/j.chroma.2015.05.005 . hal-01176925

**HAL Id: hal-01176925**

**<https://hal.science/hal-01176925>**

Submitted on 30 Sep 2015

**HAL** is a multi-disciplinary open access archive for the deposit and dissemination of scientific research documents, whether they are published or not. The documents may come from teaching and research institutions in France or abroad, or from public or private research centers.

L'archive ouverte pluridisciplinaire **HAL**, est destinée au dépôt et à la diffusion de documents scientifiques de niveau recherche, publiés ou non, émanant des établissements d'enseignement et de recherche français ou étrangers, des laboratoires publics ou privés.

1 **Potential and Limitations of On-line Comprehensive Reversed Phase Liquid**  
2 **Chromatography x Supercritical Fluid Chromatography for the Separation of**  
3 **Neutral Compounds: An approach to Separate Aqueous Extract of Bio-oil.**

4  
5 Morgan Sarrut<sup>1</sup>, Amélie Corgier<sup>1</sup>, Gérard Crétier<sup>1</sup>, Agnès Le Masle<sup>2</sup>, Stéphane  
6 Dubant<sup>3</sup>, Sabine Heinisch<sup>1\*</sup>

7  
8 <sup>1</sup> *Université de Lyon, Institut des Sciences Analytiques, UMR CNRS UCBL ENS 5280, 5 rue de la*  
9 *Doua, 69100 Villeurbanne, France*

10 <sup>2</sup> *IFP Energies nouvelles, Rond-Point de l'échangeur de Solaize, BP3, 69360 Solaize, France*

11 <sup>3</sup> *Waters SAS, BP608, 78056 St Quentin en Yvelines, France*

12 \* Corresponding author - Tel : +33(0)437 423 551 ; E-mail address : [sabine.heinisch@univ-lyon1.fr](mailto:sabine.heinisch@univ-lyon1.fr)

13  
14 **Abstract**

15  
16 On-line comprehensive Reversed Phase Liquid Chromatography x Supercritical Fluid  
17 Chromatography (RPLC x SFC) was investigated for the separation of complex  
18 samples of neutral compounds. The presented approach aimed at overcoming the  
19 constraints involved by such a coupling. The search for suitable conditions (stationary  
20 phases, injection solvent, injection volume, design of interface) are discussed with a  
21 view of ensuring a good transfer of the compounds between both dimensions, thereby  
22 allowing high effective peak capacity in the second dimension. Instrumental aspects  
23 that are of prime importance in on-line 2D separations, were also tackled (dwell  
24 volume, extra column volume and detection). After extensive preliminary studies, an  
25 on-line RPLCxSFC separation of a bio-oil aqueous extract was carried out and  
26 compared to an on-line RPLCxRPLC separation of the same sample in terms of  
27 orthogonality, peak capacity and sensitivity. Both separations were achieved in 100  
28 min. For this sample and in these optimized conditions, it is shown that RPLCxSFC  
29 can generate a slight higher peak capacity than RPLCxRPLC (620 vs 560). Such a  
30 result is essentially due to the high degree of orthogonality between RPLC and SFC

31 which may compensate for lesser peak efficiency with SFC as second dimension.  
32 Finally, in the light of the current limitations of SFC instrumentation for on-line 2D  
33 analyses, RPLCxSFC appears to be a promising alternative to RPLCxRPLC for the  
34 separation of complex samples of neutral compounds.

35

36

37

### 38 **Keywords**

39 Supercritical fluid chromatography (SFC); RPLC x SFC; Comprehensive two-  
40 dimensional chromatography; Biomass by-products

### 41 **1 Introduction**

42

43 Over the last decades, on-line comprehensive two-dimensional liquid chromatography  
44 (LCxLC) has grown significantly in many application fields [1–4]. Liquid  
45 chromatography provides a wide variety of separation modes including Reversed  
46 Phase Liquid Chromatography (RPLC), Normal Phase Liquid Chromatography  
47 (NPLC), Steric Exclusion Chromatography (SEC), Ion Exchange Chromatography  
48 (IEC) and Hydrophilic Interaction Liquid Chromatography (HILIC). On-line coupling two  
49 of these different techniques *via* an appropriate interface may produce a separation  
50 system capable of generating a very high effective peak capacity in a reasonable  
51 analysis time while avoiding sample loss and/or sample contamination [5].

52 To maximize the potential of a two-dimensional system, one of the key problems is to  
53 find orthogonal conditions between the two dimensions in order to obtain a separation  
54 that uses the largest possible fraction ( $\gamma$ ) of the separation space [6]. In this regard,  
55 NPLCxRPLC was shown to be very attractive for the separation of pharmaceutical  
56 compounds [7]. However, in spite of a lower degree of orthogonality, RPLCxRPLC has  
57 often been preferred to avoid peak deterioration associated with the incompatibility of  
58 the mobile phase of first dimension with that of second dimension (stronger eluting  
59 power or immiscibility) [2,8,9] and finally to obtain an interesting sample peak capacity  
60 for the overall comprehensive system.

61 Bio-oil samples are mainly composed of small neutral compounds. Two very recent  
62 papers [10,11] presented successful separation of aqueous bio-oil extracts by on-line  
63 RPLCxRPLC with a retention space coverage close to 50% only. NPLCxRPLC could  
64 be a possible solution to increase the utilized portion of the available space. In this  
65 work, we experiment another option which consists in coupling RPLC to supercritical  
66 fluid chromatography (RPLCxSFC). This approach was expected to be attractive  
67 because of the variety of mechanisms that govern retention in these two  
68 chromatographic systems [12]. West and Lesellier showed that polar stationary phases  
69 in SFC tend to behave as in NPLC [13]. Little polar stationary phases were also found  
70 to be attractive with SFC mobile phases as recently reported in a study which  
71 compared their use in SFC and RPLC [14]. On-line SFCxRPLC was investigated by  
72 François et al. [15] for the separation of fatty acids in fish oils and compared to on-line  
73 RPLCxRPLC for the separation of the same sample. 92 % of the separation space was  
74 occupied in SFCxRPLC versus 55 % in RPLCxRPLC. However, SFCxRPLC  
75 arrangement needed a particular interface composed of two two-position/ten-port  
76 switching valves equipped with two loops packed with octadecyl silica allowing both  
77 the depressurization of the supercritical fluid and the trapping and focusing of the  
78 analytes after an addition of water to the first dimension eluent and before the transfer  
79 to the second dimension. The potential of RPLCxSFC was highlighted by Stevenson  
80 et al. [16] in off-line mode. On-line RPLCxSFC has never been investigated yet. Here  
81 we describe our development of on-line RPLCxSFC for the separation of aromatic  
82 neutral compounds and an aqueous extract of bio-oil. With a liquid eluent in the first  
83 dimension, the interface between the two dimensions is simpler than that used in  
84 SFCxRPLC and similar to that used in RPLCxRPLC. Moreover, in the second  
85 dimension, the low viscosity of SFC mobile phase allows very fast analysis, which is of  
86 prime importance to increase peak capacity in on-line two-dimensional separations.  
87 This paper deals with the choice of SFC stationary phase, the study of phenomena  
88 resulting from the injection of a polar sample solvent into a supercritical mobile phase  
89 and the experimental and instrumental aspects related to the interface. Finally, a  
90 comparison between RPLCxSFC and RPLCxRPLC separations of the same aqueous  
91 bio-oil extract is proposed in terms of orthogonality, effective peak capacity and  
92 sensitivity.

## 94 **2 Experimental**

### 95 *2.1 Material and reagents*

96

97 Acetonitrile (ACN) (HPLC grade), methanol (MeOH) and acetone were purchased of  
98 HPLC grade from Sigma-Aldrich (Steinheim, Germany). Water was obtained from an  
99 Elga water purification system (Veolia water STI, Le Plessis Robinson, France).  
100 Pressurized liquid CO<sub>2</sub> 3.0 grade (99.9%) was obtained from Air Liquide (Pierre Bénite,  
101 France).

102 The synthetic sample for RPLCxSFC experiments was chosen among different  
103 compounds known to be representative of those found in bio-oil aqueous samples [10].  
104 It contains  $\alpha$ -hydroxycumene, phenol, 2,4,6-trimethylphenol, 1-indanone, syringol,  
105 angelica lactone, m-cresol, o-cresol, anisole, guaiacol, 5-methylfurfural and  
106 phenylethanol. They were dissolved in water/ACN 85/15 v/v at the concentration of 50  
107 mg/L. Physical properties of these twelve compounds are reported in Table 1. The  
108 compounds were either obtained from Sigma-Aldrich or graciously given by IFP  
109 Energies nouvelles (Solaize, France). The bio-oil aqueous sample was provided by  
110 IFP Energies nouvelles.

111

### 112 *2.2 Columns*

113

114 Four columns (50x2.1 mm, 1.7  $\mu$ m) from Waters (Milford, MA, USA) were used under  
115 SFC conditions : Acquity UPC<sup>2</sup> BEH-2EP, Acquity UPC<sup>2</sup> BEH, Acquity UPC<sup>2</sup> CSH  
116 Fluoro-Phenyl and Acquity UPC<sup>2</sup> HSS C18. Three columns were used under RPLC  
117 conditions : XBridge C18 (50x1.0 mm 3.5  $\mu$ m) from Waters, Hypercarb (100x1 mm, 5  
118  $\mu$ m) from Thermo Scientific (Cheshire, UK) and Acquity CSH Phenyl-Hexyl (50x2.1  
119 mm, 1.7  $\mu$ m) from Waters.

120

### 121 *2.3 Apparatus*

122

#### 123 1D-SFC system

124 Waters Acquity UPC<sup>2</sup> system was equipped with a binary solvent delivery pump, a 250  
125  $\mu\text{L}$  mixing chamber, an autosampler with a 10  $\mu\text{L}$  loop, two column ovens compatible  
126 with temperature up to 90°C and including two 6-channel column selection valves, a  
127 UV detector with a 8  $\mu\text{L}$  flow-cell and a backpressure regulator (BPR). The allowed  
128 maximum flow rate is 4 mL/min. The allowed maximum pressure is 410 bar for flow-  
129 rates up to 3.25 mL/min. This limit pressure linearly decreases to 290 bar when the  
130 flow rate increases to 4 mL/min. Data acquisition was performed by Empower software  
131 (Waters). The extra-column volume and extra-column variance were measured under  
132 liquid chromatographic conditions. They were equal to 83  $\mu\text{L}$  and 132  $\mu\text{L}^2$  respectively.  
133 The system dwell volume was estimated at 300  $\mu\text{L}$  (see section 2.4.1.).  
134

### 135 RPLCxRPLC system

136 The RPLCxRPLC system was a 2D-IClass liquid chromatograph from Waters. This  
137 instrument includes two high-pressure binary solvent delivery pumps, an autosampler  
138 with a flow-through needle of 15  $\mu\text{L}$ , a column manager composed of two column ovens  
139 with an allowed maximum temperature of 90°C and two 6-port high pressure two-  
140 position valves acting as interface between the two separation dimensions, a UV  
141 detector and a diode array detector equipped with 500 nL flow-cells. For the first  
142 dimension, the allowed maximum pressure is 1280 bar for flow-rates up to 1 mL/min ;  
143 it linearly decreases to 850 bar when flow rate increases to 2 mL/min. For the second  
144 dimension, the maximum pressure is 1280 bar for flow-rates up to 1.4 mL/min ; this  
145 limit linearly decreases to 1170 bar when flow rate increases to 2 mL/min. The  
146 measured dwell volume was 110  $\mu\text{L}$  and 120  $\mu\text{L}$  for the first and second dimensions  
147 respectively. A total extra-column volume of 12  $\mu\text{L}$  and 17  $\mu\text{L}$  and an extra-column  
148 variance of 4  $\mu\text{L}^2$  and 9  $\mu\text{L}^2$  were determined for the first and the second dimension  
149 respectively.

150 To ensure a fair comparison between RPLCxRPLC and RPLCxSFC experiments, the  
151 original interface made of two 6-port valves was replaced by a 10-port high pressure  
152 2-position valve (Vici Valco Instruments, Houston, USA) equipped with two identical  
153 loops of 20  $\mu\text{L}$ . Data acquisition, the instrumental control of the two dimensions and  
154 the programming of the 10-port high pressure 2-position valve interface were  
155 performed by Masslynx software (Waters).

156

### 157 RPLCxSFC setup

158 The first dimension consisted in the high-pressure binary solvent delivery pump, the  
159 column manager and the diode array detector of the 2D-IClass apparatus. The second  
160 dimension consisted in the high-pressure binary solvent delivery pump, the UV  
161 detector and the BPR of the Acquity UPC<sup>2</sup> apparatus, set at 140 bar.

162 As in RPLCxRPLC, the 10-port high pressure 2-position valve was used as interface  
163 between the two dimensions. It was equipped with two identical loops of 3 or 5  $\mu\text{L}$ . A  
164 30 cmx175  $\mu\text{m}$  i.d. tubing was used between the mixer of SFC pump and the 10-port  
165 2-position valve. A 56 cmx175  $\mu\text{m}$  i.d. tubing was connected between the valve and  
166 the 31.8 cmx175  $\mu\text{m}$  i.d. preheater of the second dimension column. Finally, the UV  
167 detector was connected to the column outlet by 30 cm x 175  $\mu\text{m}$  i.d. tubing.  
168 Instrumental characteristics were determined for the SFC second dimension : 300 $\mu\text{L}$   
169 for the dwell volume, , 57  $\mu\text{l}$  for the extra-column volume and 50 $\mu\text{L}^2$  for the extra-column  
170 variance. The RPLCxSFC setup is presented in Figure 1.

171 Both instrument control for the first dimension and interface programming were  
172 performed by Masslynx software. Data acquisition and instrument control for the  
173 second dimension were performed by Empower software dedicated to Acquity UPC<sup>2</sup>  
174 instrument. Synchronization between both dimensions was obtained by connecting  
175 electrically the two systems and by using external events in the first dimension method  
176 controlled by Masslynx software.

177

## 178 2.4 Chromatographic procedures

179

### 180 1D-SFC

181 In LC the dwell volume,  $V_D$ , is usually determined from a gradient experiment  
182 performed without column using MeOH as solvent A and MeOH + 0.1% acetone as  
183 solvent B. The gradient is programmed on a wide range of composition, typically from  
184 1 to 99% B, in order to minimize the uncertainty on  $V_D$  value. This latter is obtained by  
185 multiplying the measured dwell time,  $t_D$ , by the flow rate used to perform the gradient  
186 experiment.  $t_D$  is calculated from the time,  $t^*$ , corresponding to the half-part of the UV  
187 signal between the start and the end of the gradient (  $t_D = t^* - t_G / 2$ ,  $t_G$  being the  
188 gradient time). For  $V_D$  determination, SFC mobile phases are composed with CO<sub>2</sub> as  
189 solvent A and MeOH + 0.1% acetone as solvent B. It was found that when the initial  
190 composition of the programmed gradient was rich in CO<sub>2</sub> (e.g. 1 %B), the obtained

191 gradient profile was not perfectly linear, which led to a high uncertainty  $\Delta t$  on the  
192 gradient middle time  $t^*$  and consequently on the dwell volume  $V_D$  (Fig. 2a). From the  
193 experiment shown in Fig.2a,  $V_D$  was in fact estimated at  $600 \pm 300 \mu\text{L}$ . This abnormal  
194 behavior is likely to be due to the supercritical nature of the mobile phase at high  
195 percentages of  $\text{CO}_2$ . In order to correctly assess  $V_D$  in SFC, the gradient was therefore  
196 started with a higher percentage of MeOH + 0.1% acetone (i.e. 69% B) in order to get  
197 a quasi-liquid phase since the beginning of the gradient. Under these conditions the  
198 observed gradient profile was actually linear as shown in Fig. 2 b and thus, the dwell  
199 volume measurement was much more reliable (i.e.  $300 \pm 40 \mu\text{L}$ ).

200 The compatibility of the four SFC stationary phases (Acquity UPC<sup>2</sup> HSS C18, Acquity  
201 UPC<sup>2</sup> CSH FP, Acquity UPC<sup>2</sup> BEH and Acquity UPC<sup>2</sup> BEH-2EP) with LC injection  
202 solvents composed of different water/ACN proportions was tested in isocratic  
203 conditions, namely 95/2.5/2.5  $\text{CO}_2$ /MeOH/CAN. The temperature, the flow rate, the  
204 BPR, the wavelength and the sampling rate were set at 45 °C, 2.7 mL/min, 140 bar,  
205 215 nm (compensation from 350 to 450 nm) and 40 Hz respectively for all the  
206 experiments. The effect of injection solvent composition on the peak shape of o-cresol  
207 was only studied with the Acquity UPC<sup>2</sup> BEH-2EP column. The flow rate was set at 2.2  
208 mL/min. Other conditions were those mentioned above.

#### 209 RPLCxSFC

210 RPLCxSFC experiments related to the effect of RPLC solvent injection on pressure  
211 increase in second dimension were performed with the following conditions. In first  
212 dimension, X-Bridge BEH C18 column was used with mobile phase consisted in Water  
213 (A) and ACN (B); the gradient profile was : 0 min, 1% B; 29.3 min, 55% B; 31.05 min,  
214 1% B; 55 min, 1% B; the flow rate was 10  $\mu\text{L}/\text{min}$ . In second dimension Acquity UPC<sup>2</sup>  
215 CSH FP and Acquity UPC<sup>2</sup> BEH were used at 2.0 mL/min and 2.6 mL/min respectively  
216 in isocratic conditions, namely  $\text{CO}_2$ /MeOH/ACN 95/2.5/2.5 (v/v/v) at 45 °C and 140 bar  
217 as BPR. The sampling time was 0.3 min. The loop volume of the interface was 3  $\mu\text{L}$ .

218 The conditions of the RPLCxSFC separation of both synthetic sample and aqueous  
219 bio-oil extract are given in Tables 2 and 3 respectively.

#### 220 RPLCxRPLC

221 The conditions of the RPLCxRPLC separation of aqueous bio-oil extract are given in  
222 Table 3.



### 223 3 Calculations

224

225 The experimental sample peak capacities were calculated according to

$$226 \quad j_n = \frac{t_n - t_1}{w} \quad (1)$$

227  $t_n$  and  $t_1$  are the retention times of the most and the least retained compound  
228 respectively and  $w$  is the average  $4\sigma$  peak width (13.4% of peak height). Exponent  $j$   
229 stands for the dimension number.

230

231 Effective sample peak capacities were calculated by the following relationship [10]:

$$232 \quad n_{2D, effective} = \alpha \cdot n \cdot (1 - \gamma) + \gamma \cdot (\alpha \cdot n \cdot n) \quad (2)$$

233  $\gamma$  is the correction factor corresponding to the ratio of the practical to the theoretical  
234 retention area. Its calculation is detailed in reference [6].  $\alpha$  is the undersampling rate  
235 introduced by Davis et al. [17] :

$$236 \quad \alpha = \frac{1}{\sqrt{1 + 0.21 \left(\frac{6}{\tau}\right)^2}} \quad (3)$$

237 where  $\tau$  is the sampling rate of the 2D-separation (i.e. the number of fractions sent to  
238 2D per  $6\sigma$  peak width in 1D).

239

240 2D-data were processed using calculation tools developed under Excel 2007 and  
241 Matlab V7.12.0635.

242

### 243 4 Results and discussion

#### 244 4.1 Theoretical considerations

245

246 The peak capacity in the second dimension  $n^2$  increases with the ratio of the gradient  
247 time to the column dead time,  $t_G/t_0$ . It is important to note that the increase in  $n^2$  can  
248 be significant in the range of low  $t_G/t_0$  values which are usually considered in the

249 second dimension. It is therefore of prime importance to do everything possible to  
250 enhance this ratio. As previously discussed [4], this ratio can be expressed by

251

$$252 \quad \frac{{}^2t_G}{{}^2t_0} = \frac{t_s}{{}^2t_0} - \left[ \frac{{}^2V_D}{{}^2V_0} + (1+x) \right] \quad (4)$$

253 where  $t_s$  is the sampling time,  ${}^2V_D$  is the  ${}^2D$  dwell volume,  ${}^2V_0$  is the  ${}^2D$  column dead  
254 volume and  $x$  is the number of column volume required for  ${}^2D$  column equilibration  
255 between two gradient runs.

256 Eq. (4) highlights the need for (i) low  ${}^2t_0$  and therefore the use of a short  ${}^2D$  column  
257 providing high efficiency i.e. packed with sub  $2\mu\text{m}$  particles and/or the use of a high  
258 linear velocity as that usually required under SFC conditions, (ii) low  ${}^2V_D/{}^2V_0$  which is  
259 not favorable for SFC as second dimension because a rather large dwell volume is  
260 present in the current SFC instrumentation, (iii) few column volumes to equilibrate the  
261  ${}^2D$  column (i.e. low  $x$  value) and (iv) a substantial sampling time  $t_s$ . However  $t_s$  affects  
262 the injection volume in  ${}^2D$ ,  ${}^2V_i$ , according to

$$263 \quad {}^2V_i = t_s \times {}^1F \quad (5)$$

264 Where  ${}^1F$  is the flow-rate in  ${}^1D$ .

265 Critical injection effects have been reported under SFC conditions, especially when  
266 using polar injection solvents and/or large injection volumes [18,19]. With RPLC as first  
267 dimension, the injection solvent in  ${}^2D$  is composed of water and an organic solvent,  
268 typically ACN. To the best of our knowledge, no study has been devoted to hydro-  
269 organic mixtures as injection solvents in SFC. Thus, the two following sections present  
270 a thorough study to determine the maximum injection volume depending on both  
271 mobile phase composition in  ${}^1D$  and stationary phase in  ${}^2D$ .

272 In order to minimize  ${}^2V_i$  and since flow-splitting is impossible between the first RPLC  
273 dimension and the second SFC dimension to avoid  $\text{CO}_2$  depressurization when the  
274 valve is switched,  ${}^1F$  was set at the lowest value ( $10 \mu\text{L}/\text{min}$ ) recommended in gradient  
275 elution for the UHPLC instrument. As a result a  $1\text{mm}$  i.d. column was found to be the  
276 most appropriate column geometry for the first dimension.

277

#### 278 *4.2 Effect of injection of a large water volume on inlet pressure increase*

279

280 In SFC, when the injection solvent contains water, we observed a pressure increase  
281 (denoted  $\Delta P$ ) which occurs a few seconds after the injection process. Then, the  
282 pressure slowly decreases to its initial value. This phenomenon is shown in Fig.3a for  
283 1D-SFC conditions and in Fig.3b for a <sup>2</sup>D run in RPLC x SFC conditions. The injection  
284 process is different between these two configurations. In 1D-SFC, the sample is  
285 pressurized before injection thanks to a particular design of the UPC<sup>2</sup> injection system.  
286 This pressurization step results in an immediate sharp pressure increase followed by  
287 a sharp decrease down to the working pressure. In RPLC x SFC the injection system  
288 of the UPC<sup>2</sup> instrument is not used. The sample is sent from the <sup>1</sup>D RPLC column to  
289 the sample loop and then injected in the SFC <sup>2</sup>D column when the 10-port valve is  
290 switched. As a result, the preceding sharp increase does not occur. However, in both  
291 cases, the same pressure increase  $\Delta P$  can be observed. We have measured  $\Delta P$  under  
292 different conditions in 1D-SFC. The experiments were focused on the behavior of 4  
293 different SFC stationary phases subjected to 3 different injection volumes (1 , 5 and 10  
294  $\mu\text{L}$ ) with 3 different injection solvents differing in their water content (95%, 50% and  
295 5%). Among the four studied stationary phases, two were fairly apolar (Acquity CSH  
296 FP and Acquity HSS C18) while two were significantly polar (Acquity BEH and Acquity  
297 BEH-2EP). The obtained results, given in Fig.4, clearly show that  $\Delta P$  increases both  
298 with the injection volume and with the percentage of water in the injection solvent. It is  
299 also very interesting to note that the pressure increase is markedly higher with less  
300 polar stationary phases (Figs. 4a and 4b) resulting in an inlet pressure exceeding the  
301 pressure limit authorized by the instrument for 10  $\mu\text{L}$  injected in 95 % water. In this  
302 situation,  $\Delta P$  was much higher than 80bar while it remained lower than 40bar for the  
303 two polar stationary phases (Figs. 4c and 4d). For 5  $\mu\text{L}$  injected,  $\Delta P$  is still high on less  
304 polar stationary phases compared to polar stationary phases (50 vs 5 bar at 95 % water  
305 and 10 vs 2 bar at 50%water).

306 The problem of pressure increase was found to be much more critical during a RPLC  
307 x SFC separation as highlighted in Fig.5. The inlet pressure of the <sup>2</sup>D SFC instrument  
308 was recorded when an Acquity CSH FP column (Fig.5a) and an Acquity BEH column  
309 were used in <sup>2</sup>D (Fig.5b). SFC conditions were strictly identical for both columns,  
310 except flow rate set at 2.0 mL/min and 2.6 mL/min for Acquity CSH FP and Acquity  
311 BEH respectively. The sampling time was 0.3 min. Consequently 3  $\mu\text{L}$  of liquid solvent  
312 were injected in the <sup>2</sup>D SFC column every 0.3 min. The composition of this liquid

313 injection solvent changes gradually as the gradient in the <sup>1</sup>D column progresses. This  
314 variation is easily assessed by means of the <sup>1</sup>D gradient profiles given in Figs. 5a and  
315 5b. With an apolar stationary phase (Fig.5a), whereas the inlet pressure at the time of  
316 injection was 315 bar, it reached 400 bar after 10 runs. This pressure that is very close  
317 to the instrument pressure limit was kept nearly constant during 20 minutes before  
318 slowly decreasing down to the initial inlet pressure when the percentage of water  
319 becomes lower than 70%. This phenomenon was not observed with polar stationary  
320 phases (Fig.5b). To explain this, we suggest that, unlike polar stationary phases, apolar  
321 ones are poorly wetted by injection solvents rich in water, which finally results in local  
322 change of mobile phase nature. Due to the short analysis time in the second SFC  
323 dimension (0.3 min), these successive modifications have no time to be swept away.  
324 They eventually accumulate to form a multiphase plug (composed of CO<sub>2</sub>, water,  
325 MeOH and ACN) which is more viscous than the original monophasic mobile phase  
326 (CO<sub>2</sub>-MeOH-ACN mixture).

327 In addition to this critical problem of pressure increase with apolar stationary phases  
328 which prevents from working in at high flow-rates in <sup>2</sup>D, significant baseline fluctuations  
329 are observed for the fractions that are separated during the pressure plate (Fig.2c).  
330 Conversely no baseline fluctuation is noted for fractions that are analyzed when the  
331 inlet pressure is back to normal (Fig.5e). With <sup>2</sup>D polar stationary phases the <sup>2</sup>D inlet  
332 pressure remains constant during the whole RPLC x SFC separation (Fig.5b) and no  
333 disruption of the baseline is visible whatever the considered fractions (Figs. 5d and 5f).

334 In the light of these results, it is clear that a polar stationary phase should be preferably  
335 used for the SFC second dimension. Re-injection of very low injection volumes (<1 μL)  
336 in <sup>2</sup>D could probably circumvent the problems encountered with apolar stationary  
337 phase but it should lead to quite unrealistic sampling time (< 0.1min). Another  
338 alternative would be to start the RPLC gradient with a water content lower than 70%.  
339 However this option is not possible for compounds that are poorly retained in RPLC  
340 such as small polar compounds. Considering the above results, Acquity BEH-2EP was  
341 chosen as <sup>2</sup>D SFC stationary phase for the rest of this study.

#### 342 4.3 *Effect of injection volumes and injection solvent composition on peak shapes in* 343 *1D-SFC*

344

345 in SFC, it was recently shown [19] that the injection solvent composition strongly  
346 influences peak shapes. Very polar solvents such as DMSO and MeOH were found to  
347 lead to significant peak distortions even for low injected volumes, these distortions  
348 being more pronounced for less retained compounds. Abrahamsson et al. [18] also  
349 studied the effect of various injection solvents in accordance with the stationary phase.  
350 They pointed out that injection solvent may interact with stationary phase, mobile  
351 phase and solute, thereby affecting either positively or negatively peak shape.  
352 However the effect of water as injection solvent on peak shape has never been studied  
353 neither as pure solvent, probably due to the fact that it is highly polar and not much  
354 miscible with CO<sub>2</sub>, nor combined with other solvents. Here, we have studied the impact  
355 of injected volume on peak shape when the solute is dissolved in different water/ACN  
356 mixtures. Results obtained with CO<sub>2</sub>/ACN/MEOH 95/2.5/2.5 (v/v/v) as SFC mobile  
357 phase and o-cresol as solute are shown in Fig.6. Surprisingly, when the injected  
358 volume does not exceed 5 μL (i.e. 5% of the column dead volume), a very high content  
359 of ACN in injection solvent seems to be more damaging for the peak shape than a high  
360 content of water (Figs.6a and 6b). It is possible to inject up to 5 μL of sample dissolved  
361 in a solvent containing 50 to 95% water without strong peak distortion. Obviously, for  
362 10 μL injected (Fig.6c) which represents 10% of the column dead volume, the peak  
363 shapes are very bad for all studied injection solvents. The results shown in Fig.6 also  
364 point out the retention shift that increases with both the percentage of water in the  
365 injection solvent and the injection volume. It is likely to be due to two combined effects:  
366 (i) good affinity of water for the polar sites of the stationary phase and (ii) high affinity  
367 of o-cresol for water. Consequently, when the injection plug enters the column, o-cresol  
368 interacts preferentially with the stationary phase thereby increasing retention. Such  
369 retention shift could be damaging for 2D-chromatogram reconstruction due to difficulty  
370 in peak assignment between consecutive fractions analysis. However, this problem  
371 does not really arise in RPLC x SFC since the injection solvent composition slightly  
372 varies between the 2 to 4 consecutive <sup>2</sup>D runs that are required in comprehensive two-  
373 dimensional chromatography to minimize undersampling [17].

374 In view of this study, it was decided to inject a maximum of 5μL in the second SFC  
375 dimension. Since flow splitting between <sup>1</sup>D and <sup>2</sup>D was not possible with a LCxSFC  
376 configuration, injection volume in <sup>2</sup>D was directly related to both <sup>1</sup>D flow-rate and  
377 sampling time. Accordingly, with 10μL/min as <sup>1</sup>D flow-rate, the sampling time could not  
378 be higher than 30s.

#### 380 *4.4 Application to the RPLC x SFC separation of a sample of aromatic compounds*

381  
382 In order to validate the choices made previously to carry out the on-line RPLCxSFC  
383 experiments, 12 aromatic compounds were separated. The experimental conditions  
384 are given in Table 2. The sampling time and the <sup>1</sup>D flow rate being equal to 0.5 min  
385 and 10  $\mu$ L/min respectively, two identical sample loops of 5  $\mu$ L were installed on the  
386 10-port switching valve in order to completely fill the sample loop. This configuration  
387 avoids dissolving issues as highlighted in Fig.7. When the sample loop is in inject  
388 position, it is filled with the SFC mobile phase. When the sample loop comes back in  
389 load position it is depressurized, allowing some droplets of organic modifier covering  
390 the walls of the loop. Whereas this droplets can be well solubilized in the RPLC mobile  
391 phase coming from <sup>1</sup>D (Fig.7a) they may cause troublesome issues with the SFC  
392 mobile phase if the sample loop is partially filled (Fig.7b). In addition the presence of  
393 air to push the sample plug can be detrimental compared to the SFC mobile phase  
394 which is better dissolved in the hydro-organic liquid solvent. The obtained RPLCxSFC  
395 separation is presented in Fig.8a. It is interesting to notice the large occupation of the  
396 retention space by the 12 compounds, underlining the great interest of this coupling in  
397 terms of orthogonality. Furthermore, as highlighted in Fig.8b showing the separation of  
398 four consecutive fractions, peak shapes are quite symmetrical as could be expected  
399 from our preliminary studies. With 0.83s as average  $4\sigma$  peak width the sample peak  
400 capacity is close to 15 in the second dimension.

401

#### 402 *4.5 Comparison of RPLC x RPLC and RPLC x SFC systems for the separation of a* 403 *bio-oil sample*

404

405 An RPLCxSFC experiment was carried out on a real sample consisting in an aqueous  
406 extract of a bio-oil. The conditions of the first dimension were similar to those used in  
407 a previous study [10] except the gradient time that is much lower in the present work.  
408 In order to elute all the compounds in <sup>2</sup>D SFC conditions, a gradient from 15% to 50 %  
409 MeOH/ACN (1:1) is needed. The contour plot of the RPLCxSFC separation is  
410 presented in Fig.9a. For comparison, Fig.9b shows the RPLCxRPLC separation of the  
411 same sample performed using the same <sup>1</sup>D conditions as the RPLCxSFC separation.

412 For a better comparison of the two separations, the sampling time was also kept  
413 identical (i.e. 30s). As a consequence,  $^1n$  and  $\alpha$  were identical for both separations.  
414 Experimental conditions are given in Table 3.

415 Fig. 9 clearly underlines that the RPLCxSFC system offers much higher degree of  
416 orthogonality ( $\gamma$  close to 1) compared to the RPLCxRPLC configuration ( $\gamma$  close to 0.6).  
417 It is important to note that this latter configuration and the corresponding conditions  
418 displayed in Table 3 were found to provide the highest effective peak capacity among  
419 the different studied RPLCxRPLC systems [10]. In RPLCxSFC, the enhancement of  
420 the available separation space allows to reach an effective peak capacity slightly  
421 higher in spite of a higher  $^2n$  with RPLCxRPLC conditions (see Table 4). Several  
422 reasons could explain why  $^2n$  is higher with RPLC as second dimension:

423 (i)  $^2t_G/2t_0$  ratio was more than three times higher for RPLCxRPLC (5.4 vs 1.7 for  
424 RPLCxSFC) leading to a higher peak capacity in second dimension according to eq.  
425 (4) and as discussed in section 4.1. Indeed, despite a  $^2t_s/2t_0$  ratio in favor of RPLCxSFC  
426 due to the higher flow rate used in SFC (2.0 mL/min vs 1.2 mL/min in RPLC), the dwell  
427 volume is larger in SFC (300  $\mu$ L vs 120  $\mu$ L in LC) increasing  $^2V_D/2V_0$  ratio. Moreover,  
428 for software reasons, an extra-time of 0.2 min had to be added between two  
429 consecutive runs of second dimension in SFC, thereby leading to a real acquisition  
430 time of only 0.3 min. As a consequence, while the number of column volumes used for  
431 column equilibration,  $x$ , was set at 2 for RPLC as second dimension,  $x$  was equal to 4  
432 for SFC, which therefore significantly decreased  $^2t_G/2t_0$  ratio. It was shown that only two  
433 column dead volumes ( $x=2$ ) can provide a good run-to-run repeatability in UHPLC  
434 conditions [20–22] which was also found to be suitable for SFC conditions for neutral  
435 compounds (data not shown).

436 (ii) The extra-column variance is markedly higher with SFC apparatus compared to  
437 UHPLC apparatus and led to an important loss of efficiency especially for 50x2.1 mm  
438 column [23]. In our case the extra-column variance in 2D was 3.5 times larger in  
439 RPLCxSFC (32  $\mu$ L<sup>2</sup> vs 9  $\mu$ L<sup>2</sup> in RPLCxRPLC). This is mainly due to both larger tubing  
440 i.d. and larger flow-cell volume of the UV detector used in SFC (175  $\mu$ m and 16  $\mu$ L  
441 respectively) compared to those used in RPLC (65  $\mu$ m and 0.5  $\mu$ L respectively).

442 (iii) Some significant injection effects still exist in RPLCxSFC whereas none were  
443 observed in RPLCxRPLC. The compatibility of the mobile phases of the two  
444 dimensions is more challenging in RPLCxSFC which may involve more critical injection  
445 effects. Moreover, while all the peaks in the  $^2$ D RPLC have nearly the same width (i.e.

446 0.6s), the peak shapes obtained in <sup>2</sup>D SFC were not similar with  $w_{4\sigma}$  varying from 0.51  
447 s to 1.50 s depending on the compounds. As a result the average measured peak width  
448 at  $4\sigma$  was 0.60 s in RPLC compared to 1.09 s in SFC conditions. More pronounced  
449 injection effects, resulting in a loss of column efficiency, could also probably explain  
450 the 7-fold loss in sensitivity when using SFC as second dimension compared to RPLC  
451 making RPLCxSFC less attractive in terms of sensitivity.  
452 Finally, despite the raised instrumental issues, the present results show that  
453 RPLCxSFC can be a good alternative to RPLCxRPLC for the separation of biomass  
454 by-products

455

## 456 **5 Conclusions**

457

458 The goal of this work was to evaluate the potential of on-line RPLCxSFC for the  
459 separation of aromatic compounds. Suitable stationary phase and injection volume for  
460 the <sup>2</sup>D SFC were chosen thanks to preliminary studies aiming at overpassing the lack  
461 of compatibility between the mobile phases used as first and second dimension. Polar  
462 stationary phases in SFC seem to be the most adapted stationary phases. On the other  
463 hand it was shown that a maximum of 5  $\mu$ L of a mixture of water/acetonitrile was  
464 appropriate to inject in the second SFC dimension. An on-line RPLCxSFC separation  
465 of a real aqueous bio-oil sample was successfully carried out achieving full  
466 orthogonality ( $\gamma=1$ ), while with an optimized RPLCxRPLC separation  $\gamma$  could not  
467 exceed 0.59. Accordingly, although wider peaks were observed in SFC as second  
468 dimension, the effective peak capacity was slightly higher with RPLCxSFC  
469 configuration (620 vs 560 with RPLCxRPLC). However, it should be noted that the  
470 peak capacity in <sup>2</sup>D SFC was limited by the high dwell volume of the apparatus as well  
471 as software issues due to this unusual coupling. Consequently, we are sure that there  
472 is still room for further improvements. Yet, sensitivity was found markedly higher with  
473 the RPLCxRPLC separation due to an important extra-column variance with the SFC  
474 system and still pronounced injection effects in SFC. Finally, in the light of these  
475 results, on-line RPLCxSFC can be considered as an interesting alternative for the  
476 separation of neutral compounds compared to RPLCxRPLC.

477

## 478 **Acknowledgements**



479

480 M.S., S.H. and G.C. wish to thank Waters for the loan of the UPC<sup>2</sup> system and  
481 especially Philippe Mériquier for his help in LCxSFC setting up. S.H. would like to thank  
482 Davy Guillaume for stimulating discussions and valuable advice on different aspects of  
483 SFC.

484

485

- 486 [1] P. Dugo, F. Cacciola, T. Kumm, G. Dugo, L. Mondello, *J. Chromatogr. A* 1184  
487 (2008) 353.
- 488 [2] I. François, K. Sandra, P. Sandra, *Anal. Chim. Acta* 641 (2009) 14.
- 489 [3] P.Q. Tranchida, P. Donato, F. Cacciola, M. Beccaria, P. Dugo, L. Mondello, *TrAC*  
490 *Trends Anal. Chem.* 52 (2013) 186.
- 491 [4] M. Sarrut, G. Crétier, S. Heinisch, *TrAC Trends Anal. Chem.* 63 (2014) 104.
- 492 [5] G. Guiochon, N. Marchetti, K. Mriziq, R.A. Shalliker, *J. Chromatogr. A* 1189  
493 (2008) 109.
- 494 [6] A. D'Attoma, C. Grivel, S. Heinisch, *J. Chromatogr. A* 1262 (2012) 148.
- 495 [7] I. François, A. De Villiers, P. Sandra, *J. Sep. Sci.* 29 (2006) 492.
- 496 [8] K.J. Mayfield, R.A. Shalliker, H.J. Catchpole, A.P. Sweeney, V. Wong, G.  
497 Guiochon, *J. Chromatogr. A* 1080 (2005) 124.
- 498 [9] P. Jandera, *J. Sep. Sci.* 29 (2006) 1763.
- 499 [10] A. Le Masle, D. Angot, C. Gouin, A. D'Attoma, J. Ponthus, A. Quignard, S.  
500 Heinisch, *J. Chromatogr. A* 1340 (2014) 90.
- 501 [11] D. Tomasini, F. Cacciola, F. Rigano, D. Sciarrone, P. Donato, M. Beccaria, E.B.  
502 Caramão, P. Dugo, L. Mondello, *Anal. Chem.* 86 (2014) 11255.
- 503 [12] G. Guiochon, A. Tarafder, *J. Chromatogr. A* 1218 (2011) 1037.
- 504 [13] C. West, E. Lesellier, *J. Chromatogr. A* 1110 (2006) 191.
- 505 [14] A. Grand-Guillaume Perrenoud, J.-L. Veuthey, D. Guillaume, *J. Chromatogr. A*  
506 1266 (2012) 158.
- 507 [15] I. François, P. Sandra, *J. Chromatogr. A* 1216 (2009) 4005.
- 508 [16] P.G. Stevenson, A. Tarafder, G. Guiochon, *J. Chromatogr. A* 1220 (2012) 175.
- 509 [17] J.M. Davis, D.R. Stoll, P.W. Carr, *Anal. Chem.* 80 (2008) 461.
- 510 [18] V. Abrahamsson, M. Sandahl, *J. Chromatogr. A* 1306 (2013) 80.
- 511 [19] J.N. Fairchild, J.F. Hill, P. Iraneta, *LC-GC N. Am.* 31 (2013) 326.
- 512 [20] A.P. Schellinger, D.R. Stoll, P.W. Carr, *J. Chromatogr. A* 1192 (2008) 41.
- 513 [21] A.P. Schellinger, D.R. Stoll, P.W. Carr, *J. Chromatogr. A* 1192 (2008) 54.
- 514 [22] C. Grivel, J.-L. Rocca, D. Guillaume, J.-L. Veuthey, S. Heinisch, *J. Chromatogr.*  
515 *A* 1217 (2010) 459.
- 516 [23] A. Grand-Guillaume Perrenoud, C. Hamman, M. Goel, J.-L. Veuthey, D.  
517 Guillaume, S. Fekete, *J. Chromatogr. A* 1314 (2013) 288.

518

519 Figure captions :

520 Figure 1 : RPLCxSFC setup. (a) The eluent of first dimension is stored in loop 1 while  
521 the content of loop 2 is injected in second dimension and (b) vice versa

522 Figure 2 : Influence of gradient profile on the dwell volume measurement in SFC.  
523 Mobile phases : A=CO<sub>2</sub>, B=MeOH+0.1% acetone. Temperature = 30 °C. BPR = 140  
524 bar. Detection Wavelength = 254 nm. Programmed gradient : (a) 1-99 %B in 8 min at  
525 1 mL/min, (b) 69-99 %B in 3 min at 1.5 mL/min. Dotted lines are the tangents to the  
526 obtained gradient profile.  $\Delta t$  represents the uncertainty at half part of the UV signal with  
527  $t^*$  being the corresponding time.

528 Figure 3 : Observed inlet pressure of the SFC instrument vs run time in (a) 1D-SFC  
529 and (b) RPLC x SFC. Conditions common to all experiments : injection solvent =  
530 Water/ACN 95/5 (v/v) ; mobile phase = CO<sub>2</sub>/MeOH/ACN 95/2.5/2.5 (v/v/v) ; column =  
531 Acquity UPC<sup>2</sup> CSH FP 50x2.1 mm, 1.7  $\mu$ m ; temperature = 45°C ; BPR = 140 bar.  
532 Other conditions : (a) flow rate = 2.7 mL/min, injected volume = 5  $\mu$ L ; (b) flow rate =  
533 2.0 mL/min, injected volume = 3  $\mu$ L.  $\Delta P$  represents the pressure increase (see text for  
534 more details)

535 Figure 4 : Pressure increase  $\Delta P$  in 1D-SFC as a function of water content of the  
536 injection solvent and injection volume  $V_i$  on (a) Acquity UPC<sup>2</sup> CSH FP column, (b),  
537 Acquity UPC<sup>2</sup> HSS C18 column, (c) Acquity UPC<sup>2</sup> BEH column and (d) Acquity UPC<sup>2</sup>  
538 BEH-2EP column. Column geometry : 50x2.1 mm, 1.7  $\mu$ m ; flow rate = 2.7 mL/min ;  
539 temperature = 45°C ; BPR = 140 bar ; injection solvent = mixture of water and  
540 acetonitrile. \* means that  $\Delta P$  could not be measured because the pressure limit (414  
541 bar) was reached.

542 Figure 5: Influence of <sup>2</sup>D stationary phase on the course of a RPLCxSFC experiment.  
543 (a) and (b) : SFC inlet pressure versus run time. c) and (d) : <sup>2</sup>D analysis of fractions  
544 eluted from <sup>1</sup>D between 20.1 and 21.0 min. (e) and (f) : <sup>2</sup>D analysis of fractions eluted  
545 from <sup>1</sup>D between 36.3 and 37.2 min. Sampling time = 0.3 min. RPLC conditions :  
546 column dimensions = 50x1.0 mm, stationary phase = 3.5  $\mu$ m Xbridge C18, solvent A  
547 = water, solvent B = ACN, gradient from 1% B to 55 % B in 29.3 min, flow rate = 10  
548  $\mu$ L/min, temperature = 30 °C. SFC conditions : column dimensions = 50x2.1 mm,  
549 stationary phase = (a,c,e) 1.7  $\mu$ m Acquity UPC<sup>2</sup> CSH FP ; (b,d,f) 1.7  $\mu$ m Acquity UPC<sup>2</sup>  
550 BEH, isocratic mobile phase = CO<sub>2</sub>/MeOH/ACN 95/2.5/2.5 (v/v/v), flow rate = (a,c,e)  
551 2.0 mL/min ; (b,d,e) 2.6 mL/min, temperature = 45 °C, BPR = 140 bar. Full lines shows

552 the gradient profile in <sup>1</sup>D outlet. Dotted lines show the time windows for the selected  
553 fractions.

554 Figure 6 : Effect of injection solvent and injected volume peak shape. Solute : o-cresol  
555 with (a) 1 $\mu$ L, (b) 5 $\mu$ L, (c) 10  $\mu$ L. Injection solvent composition: Water/ACN 95/5 (v/v)  
556 (—), 50/50 (v/v) (—) and 5/95 (v/v) (—). Column : Acquity UPC<sup>2</sup> BEH-2EP, 50x2.1  
557 mm, 1.7  $\mu$ m. Flow rate = 2.2 mL/min; mobile phase: CO<sub>2</sub>/MeOH/ACN 95/2.5/2.5 (v/v/v).  
558 Temperature = 45°C. BPR = 140 bar. Detection wavelength = 215 nm (compensation  
559 from 350 nm to 450 nm).

560 Figure 7 : schematic representation of injection process in the second dimension of  
561 RPLCxSFC with (a) completely and (b) partially filling of the loops

562 Figure 8 : On-line RPLCxSFC separation of 12 aromatic compounds. (a) contour plot  
563 UV and (b) overlay of SFC separation of the fractions from 27 min to 28.5 min (red  
564 dotted lines in the contour plot). See Table 1 for solutes and Table 3 for experimental  
565 conditions.

566 Figure 9 : Comparison (a) on-line RPLCxSFC and (b) on-line RPLCxRPLC separation  
567 of a bio-oil aqueous extract. Experimental conditions are summarized in Table 3. The  
568 red dotted lines in (b) delimit the separation space.

569

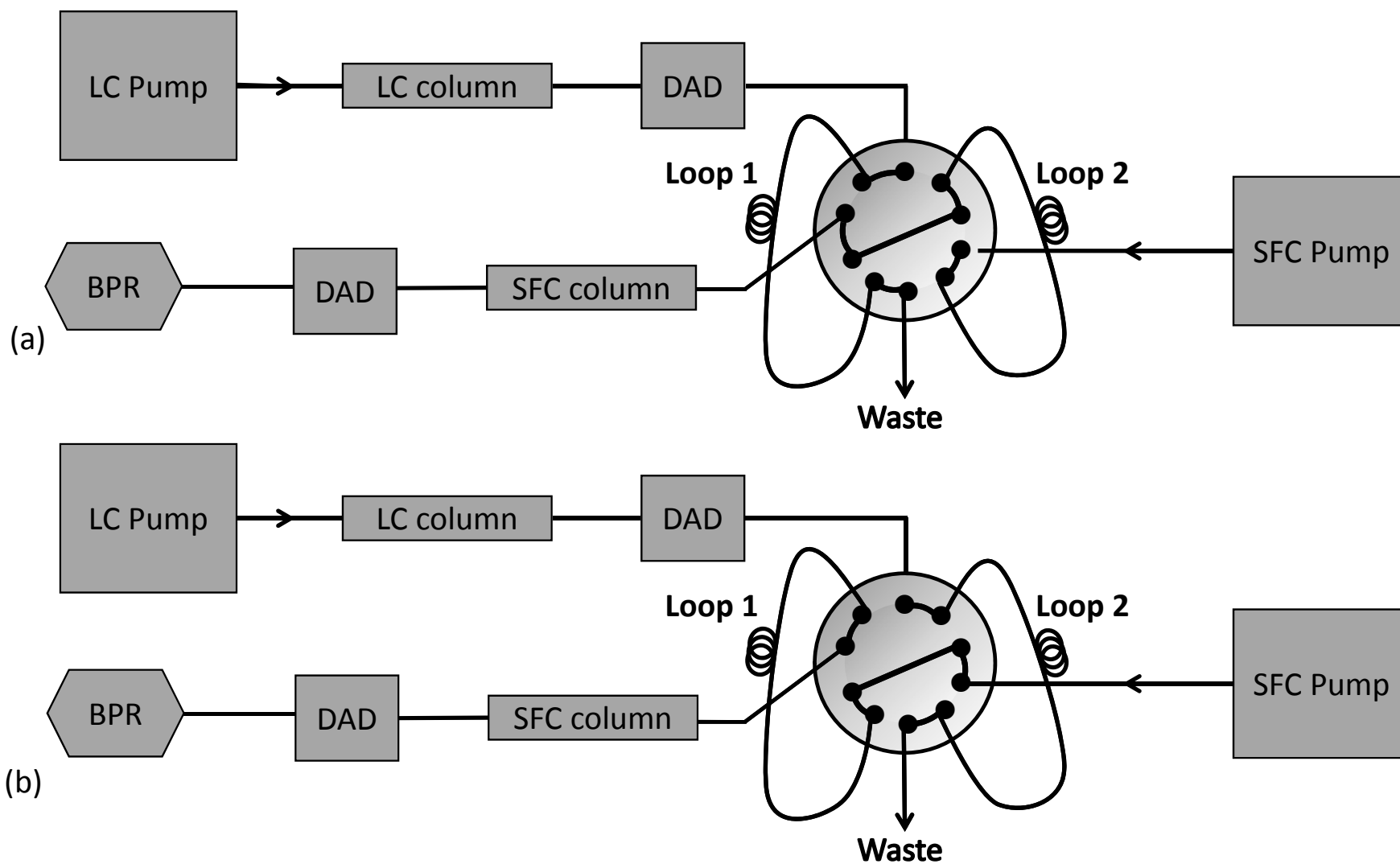


Figure 1 :

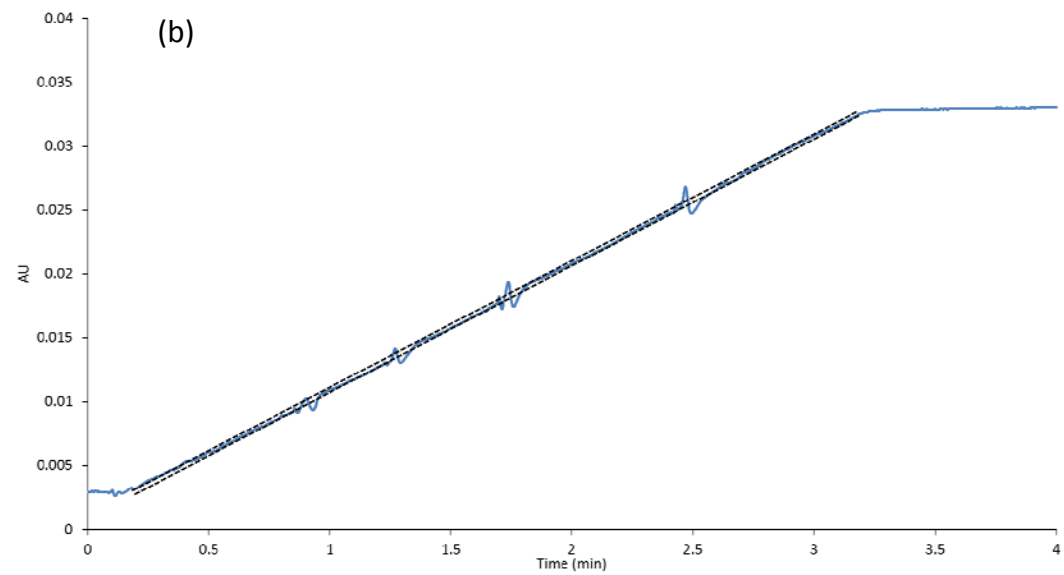
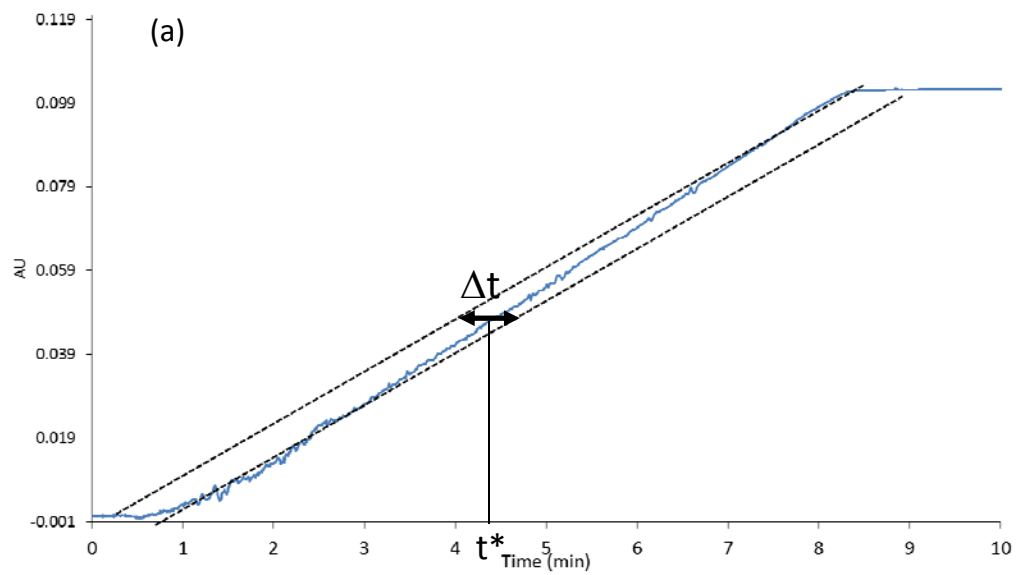


Figure 2

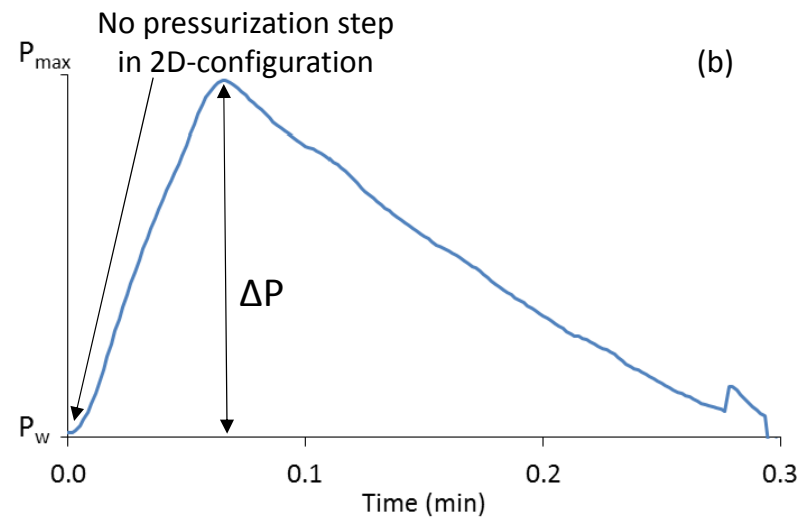
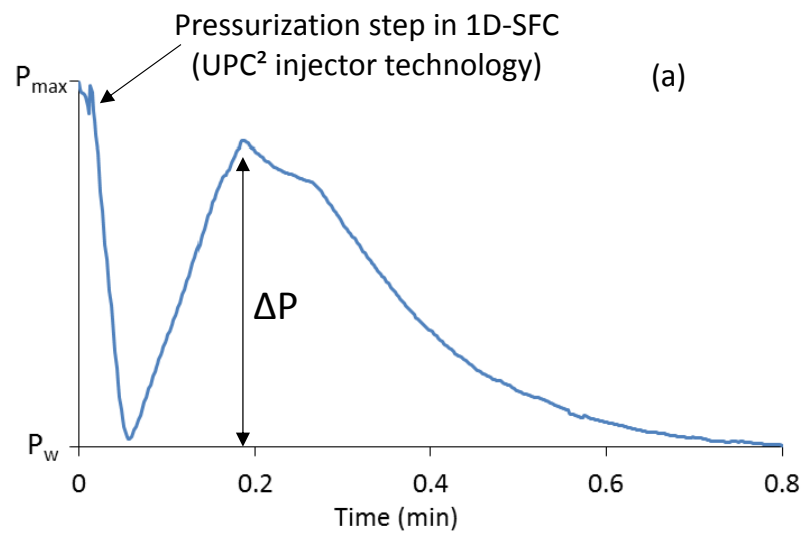


Figure 3

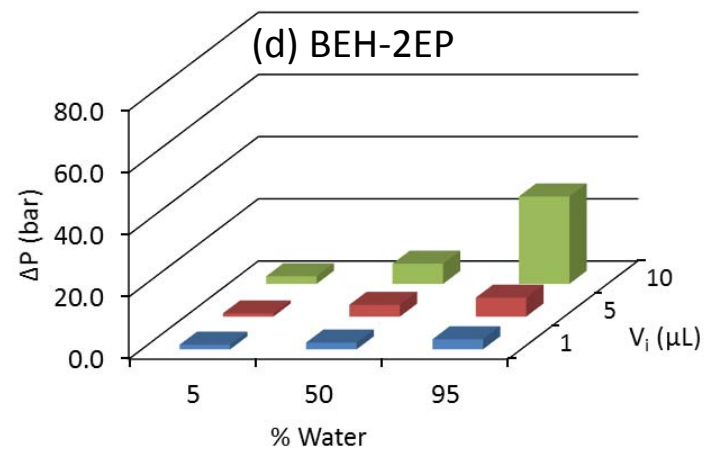
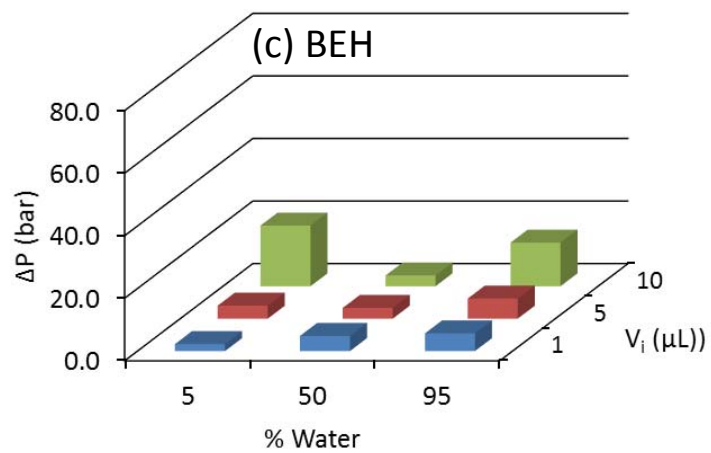
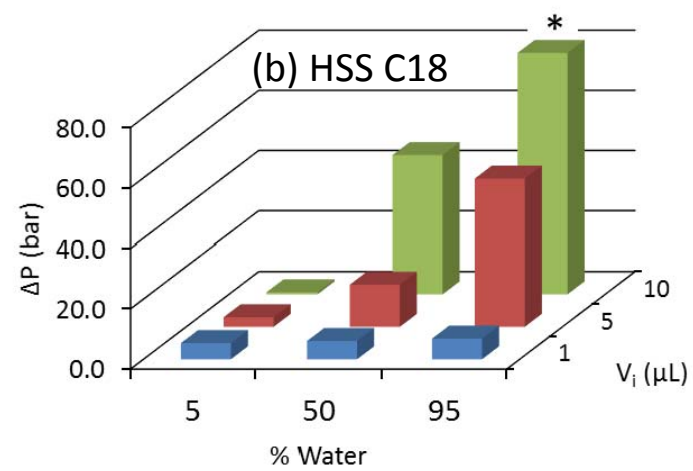
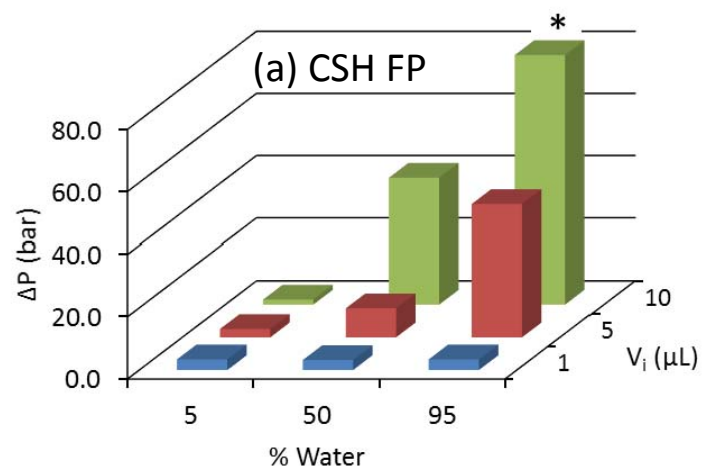


Figure 4

### CSH FP column

### BEH column

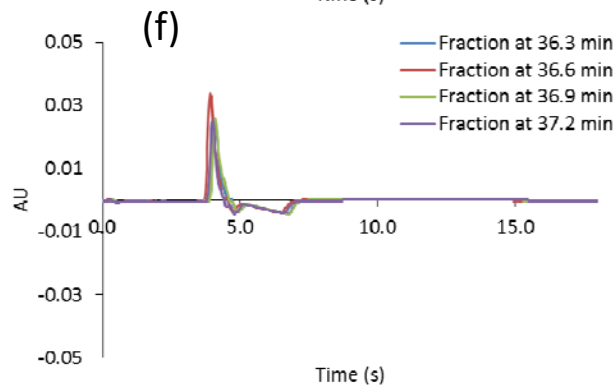
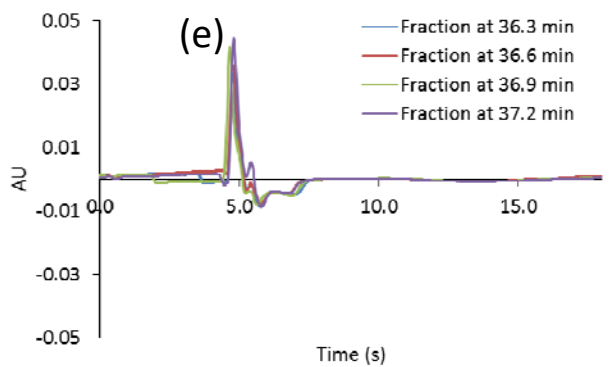
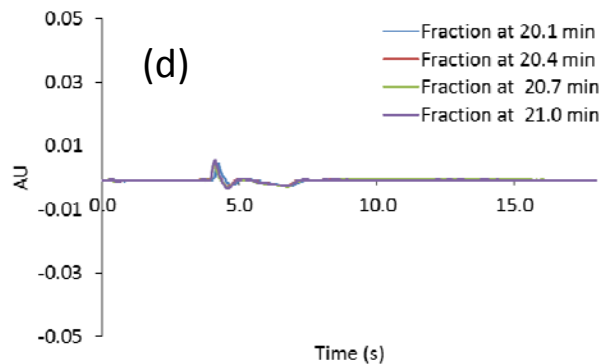
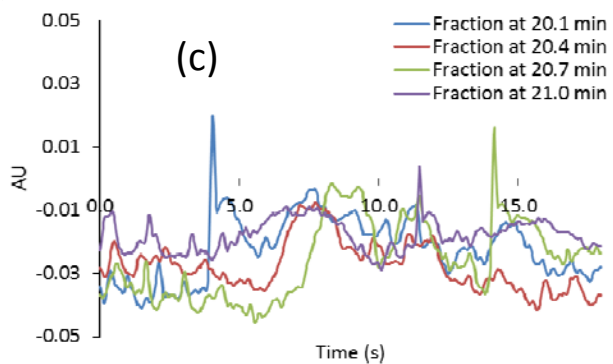
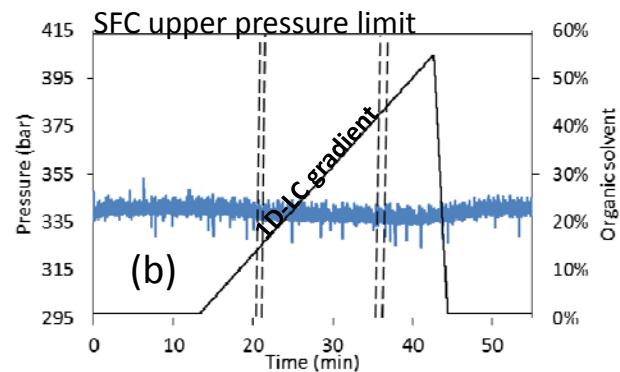
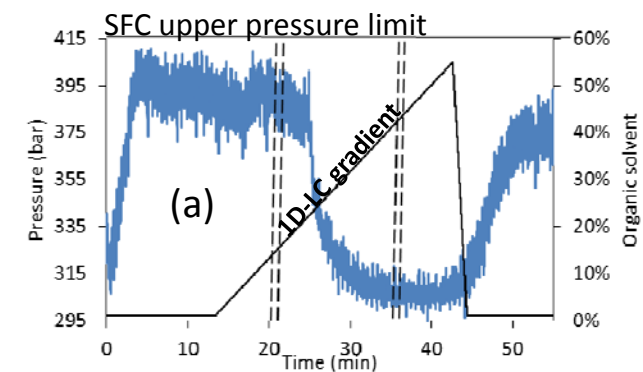


Figure 5



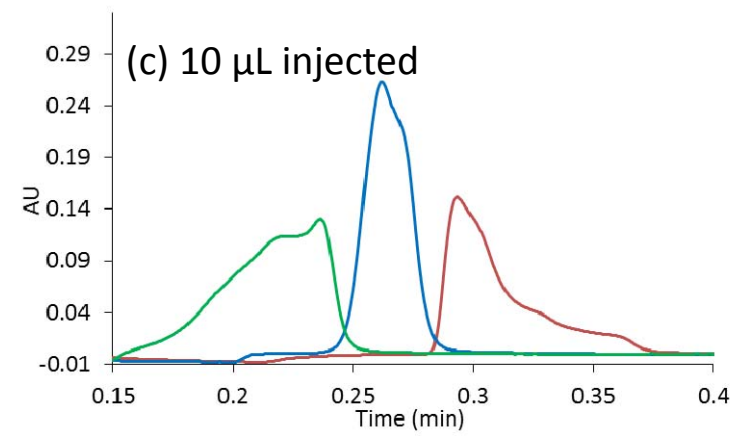
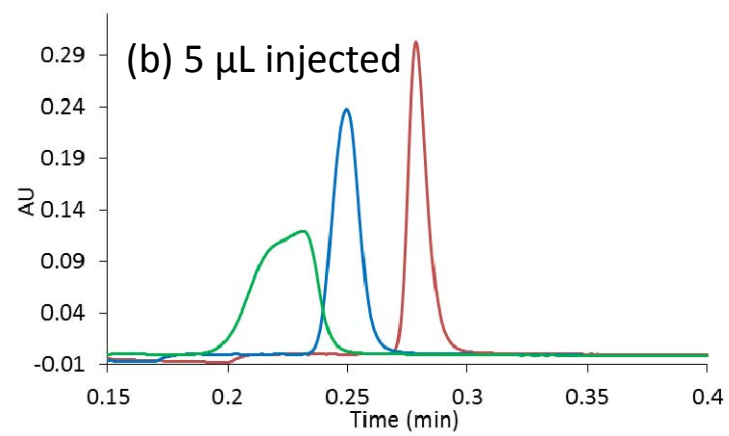
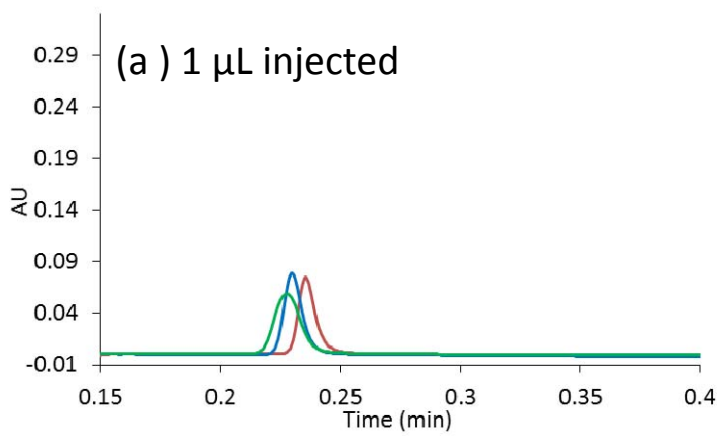


Figure 6

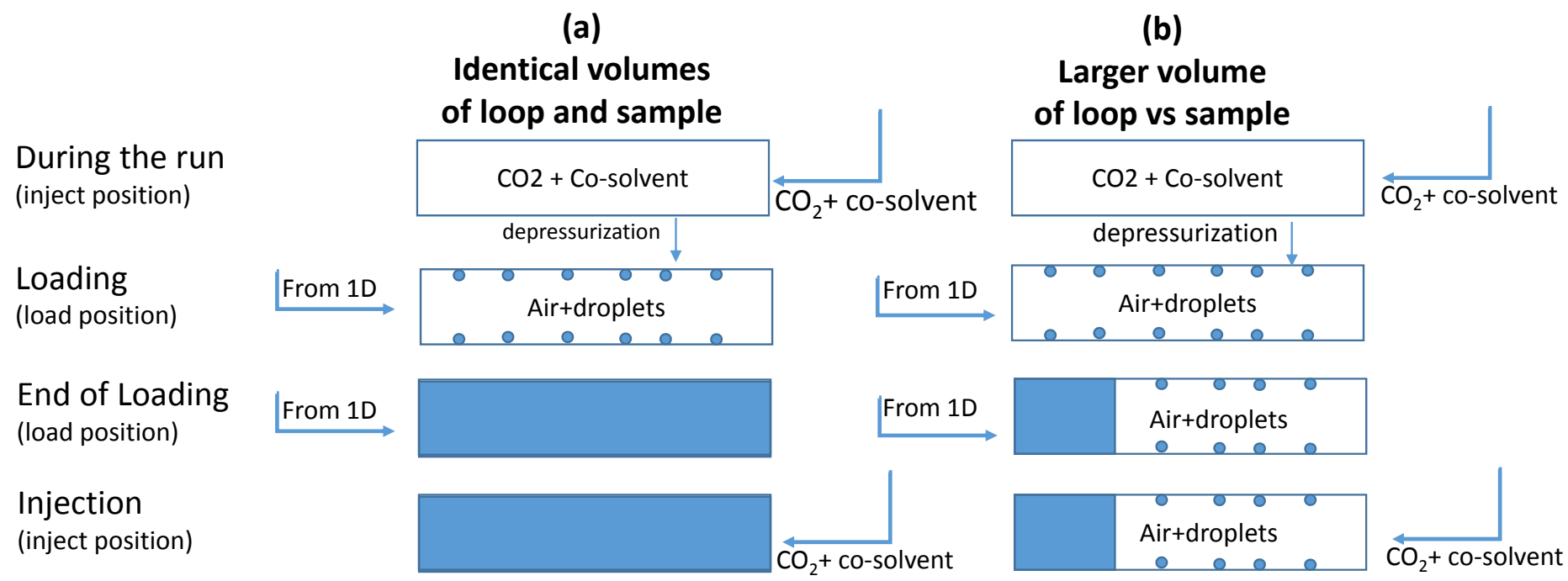


Figure 7

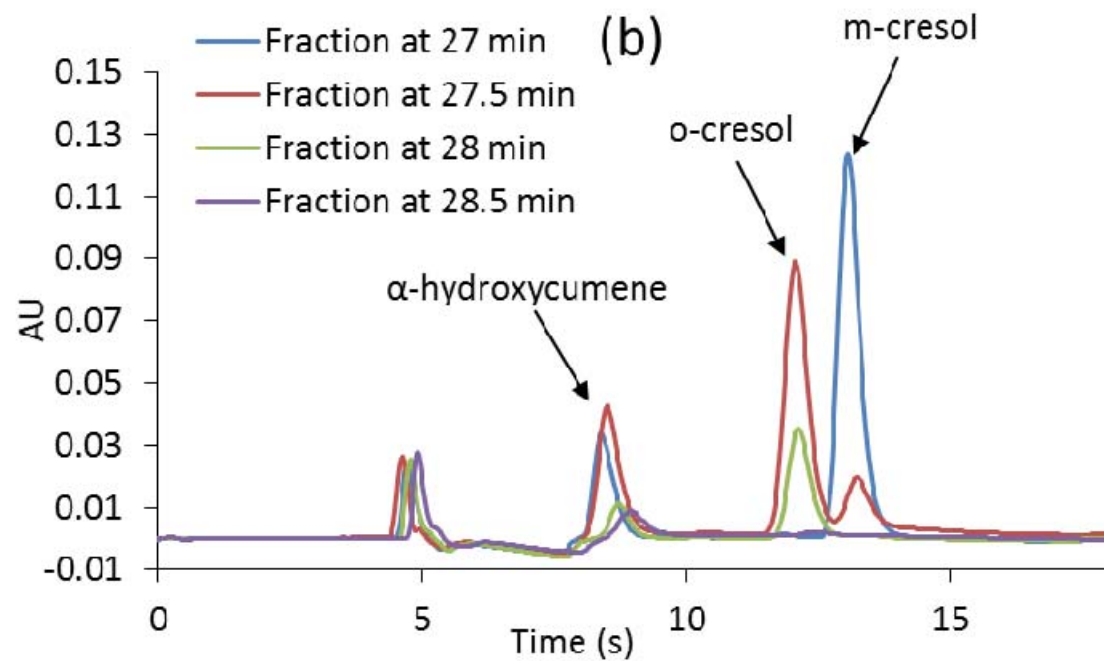
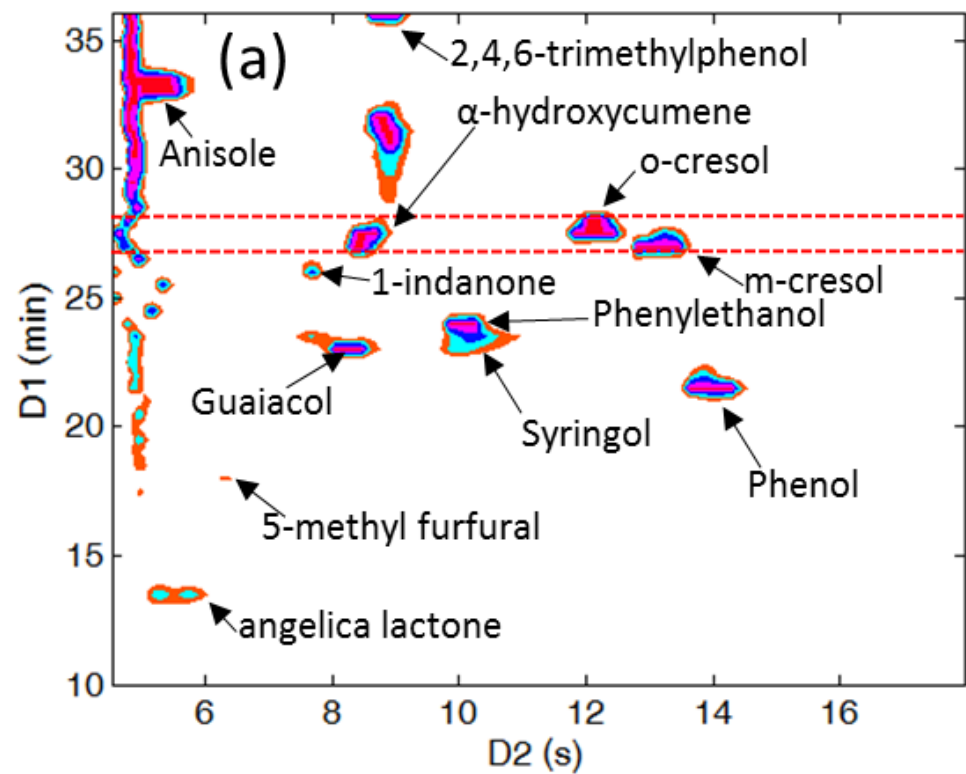
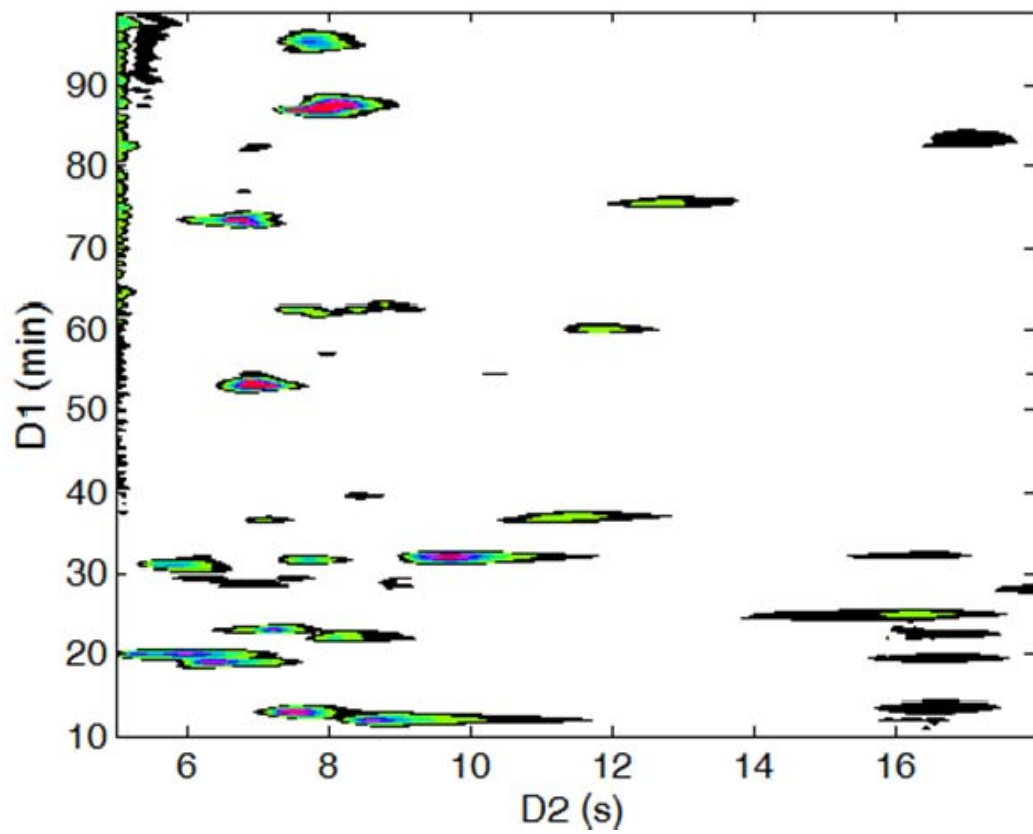


Figure 8

**(a) RPLCxSFC**



**(b) RPLCxRPLC**

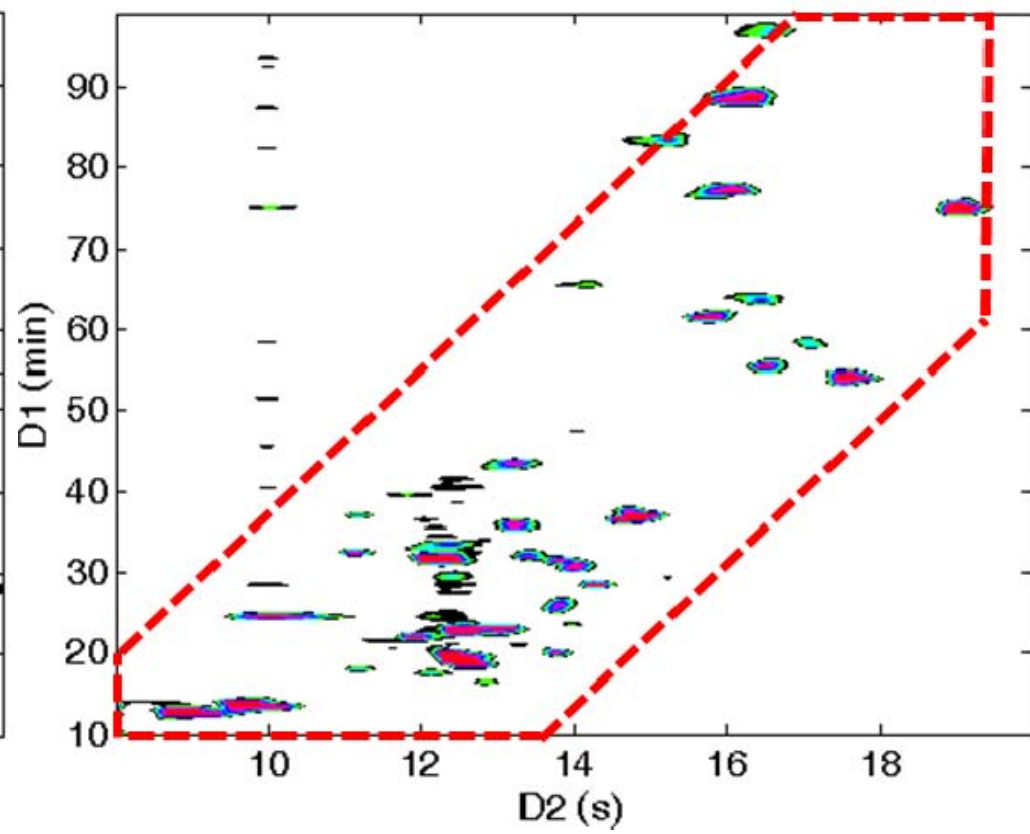


Figure 9

1 Table 1 - Physical and chemical properties of some bio-oil representative compounds

	Compound	Chemical family	Molecular Formula	MW (g/mol)	log P
1	$\alpha$ -angelica lactone	lactone	C <sub>5</sub> H <sub>6</sub> O <sub>2</sub>	98.10	0.236
2	2-phenylethanol	alcohol	C <sub>8</sub> H <sub>10</sub> O	122.16	1.504
3	5-methylfurfural	furan	C <sub>6</sub> H <sub>6</sub> O <sub>2</sub>	110.11	0.670
4	phenol	phenol	C <sub>6</sub> H <sub>6</sub> O	94.11	1.540
5	o-cresol	phenol	C <sub>7</sub> H <sub>8</sub> O	108.14	1.962
6	m-cresol	phenol	C <sub>7</sub> H <sub>8</sub> O	108.14	2.043
7	2,4,6-trimethylphenol	phenol	C <sub>9</sub> H <sub>12</sub> O	136.19	2.935
8	$\alpha$ -hydroxycumene	phenol	C <sub>9</sub> H <sub>12</sub> O	136.19	2.861
9	guaiacol	guaiacol	C <sub>7</sub> H <sub>8</sub> O <sub>2</sub>	124.14	1.341
10	syringol	syringol	C <sub>8</sub> H <sub>10</sub> O <sub>3</sub>	154.16	1.218
11	1-indanone	enone	C <sub>9</sub> H <sub>8</sub> O	132.16	1.419
12	anisole	aromatic ether	C <sub>7</sub> H <sub>8</sub> O	108.14	2.170

- 1 Table 3 – Experimental conditions for both RPLCxSFC and RPLCxRPLC separations  
 2 of the bio-oil aqueous sample

	RPLC ( <sup>1</sup> D)	SFC ( <sup>2</sup> D)	RPLC ( <sup>2</sup> D)
Stationary phase	Hypercarb	Acquity UPC <sup>2</sup> BEH-2EP	Acquity CSH Phenyl Hexyl
Column geometry	100x1.0 mm, 5 μm	50x2.1 mm, 1.7 μm	50x2.1 mm, 1.7 μm
Mobile phase	A : Water B : ACN	A : CO <sub>2</sub> B : MeOH/ACN 1:1 (v/v)	A : Water + 0.1 % FA* B : ACN + 0.1 % FA
Flow rate	10 μL/min	2 mL/min	1.2 mL/min
Gradient	5 to 99 % (B) in 102.5 min	15 to 50% (B) in 0.12 min	5 to 55% (B) in 0.18 min
BPR	/	140 bar	/
Temperature	30 °C	45 °C	80 °C
UV	220 nm	220 nm Compensation from 350 to 450 nm	220 nm
Injected volume	5 μL	5 μL	5 μL

3 0.5 min as sampling time

4 \* FA means formic acid

- 1 Table 2 – Experimental conditions for the RPLCxSFC separation of the 12  
 2 representative compounds (see list in table 1)

	RPLC ( <sup>1</sup> D)	SFC ( <sup>2</sup> D)
Stationary phase	X Bridge BEH C18	Acquity UPC <sup>2</sup> BEH-2EP
Column geometry	50x1.0 mm, 3.5 μm	50x2.1 mm, 1.7 μm
Mobile phase	A : Water B : ACN	A : CO <sub>2</sub> B : MeOH/ACN 1:1 (v/v)
Flow rate	10 μL/min	2 mL/min
Gradient	8 to 51 % (B) in 23 min	Isocratic 5% (B)
BPR	/	140 bar
Temperature	30 °C	45 °C
UV	220 nm	215 nm (compensation from 350 to 450 nm)
Vinj	2 μL	5 μl

- 3 0.5 min as sampling time

1 Table 4 – Experimental results of RPLCxSFC and RPLCxRPLC

	$\gamma$	$\alpha$	$^1n$	$^2W_{4\sigma}$ (s)	$^2n$	$^1n \cdot ^2n$	$n_{2D, effective}$
RPLCxSFC	1	0.85	56	1.09	13	730	620
RPLCxRPLC	0.59	0.85	56	0.60	20	1120	560

2

3  $^1n$  and  $^2n$  were calculated according to eq.1

4  $\gamma$  was calculated according [6]

5  $\alpha$  was calculated according to eq.3

6  $n_{2D, effective}$  was calculated according to eq.2